Theory for the Charge-Density-Wave Mechanism of 3D Quantum Hall Effect

Fang Qin (覃昉)[,1,2,3] Shuai Li,[1] Z. Z. Du,[1,4] C. M. Wang,[5,1,4] Wenqing Zhang,[1,3] Dapeng Yu,[1,4]
Hai-Zhou Lu,[1,4,*] and X. C. Xie[6,7,8]

[1]*Shenzhen Institute for Quantum Science and Engineering and Department of Physics,
Southern University of Science and Technology (SUSTech), Shenzhen 518055, China*
[2]*CAS Key Laboratory of Quantum Information, University of Science and Technology of China,
Chinese Academy of Sciences, Hefei, Anhui 230026, China*
[3]*Shenzhen Municipal Key-Lab for Advanced Quantum Materials and Devices, Shenzhen 518055, China*
[4]*Shenzhen Key Laboratory of Quantum Science and Engineering, Shenzhen 518055, China*
[5]*Department of Physics, Shanghai Normal University, Shanghai 200234, China*
[6]*International Center for Quantum Materials, School of Physics, Peking University, Beijing 100871, China*
[7]*CAS Center for Excellence in Topological Quantum Computation, University of Chinese Academy of Sciences,
Beijing 100190, China*
[8]*Beijing Academy of Quantum Information Sciences, West Building 3, No. 10, Xibeiwang East Road,
Haidian District, Beijing 100193, China*

The charge-density-wave (CDW) mechanism of the 3D quantum Hall effect has been observed recently in ZrTe$_5$ [Tang *et al.*, Nature **569**, 537 (2019)]. Different from previous cases, the CDW forms on a one-dimensional (1D) band of Landau levels, which strongly depends on the magnetic field. However, its theory is still lacking. We develop a theory for the CDW mechanism of 3D quantum Hall effect. The theory can capture the main features in the experiments. We find a magnetic field induced second-order phase transition to the CDW phase. We find that electron-phonon interactions, rather than electron-electron interactions, dominate the order parameter. We extract the electron-phonon coupling constant from the non-Ohmic $I - V$ relation. We point out a commensurate-incommensurate CDW crossover in the experiment. More importantly, our theory explores a rare case, in which a magnetic field can induce an order-parameter phase transition in one direction but a topological phase transition in other two directions, both depend on one magnetic field.

Introduction.—The quantum Hall effect is one of the most important discoveries in physics [1–4]. It arises from the Landau levels of two-dimensional (2D) electron gas in a strong magnetic field (Fig. 1, left). When the Fermi energy lies between two Landau levels, the interior of the electron gas is insulating but the deformed Landau levels at the edges can transport electrons dissipationlessly, leading to the quantized Hall resistance and vanishing longitudinal resistance of the quantum Hall effect. The quantum Hall effect is difficult in 3D, where the Landau levels turn to a series of 1D bands of Landau level dispersing with the momentum along the direction of magnetic field (Fig. 1, center). Because the Fermi energy always crosses some Landau bands, the interior is metallic, which buries the quantization of the edge states, so the quantum Hall effect is usually observed in 2D systems [5]. Nevertheless, searching for a 3D quantum Hall effect has been lasting for more than 30 years [6–28]. One of the famous proposals for the 3D quantum Hall effect relies on the charge density wave (CDW), which may gap the 1D Landau band so that the bulk is insulating. In real space, the CDW splits the 3D
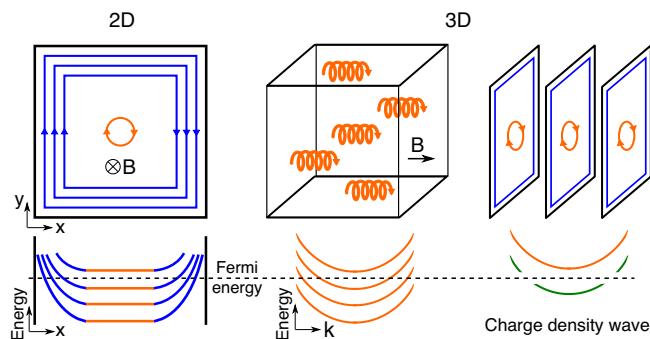

FIG. 1. Left: in 2D, the quantum Hall effect arises when only the edge states (blue) conduct electrons, while the interior bulk states are insulating as the Fermi energy lies between the Landau levels. Center: in 3D, the Landau levels turn to 1D bands of Landau levels that disperse with the momentum (k) along the direction of magnetic field. The quantum Hall effect is difficult in 3D because the bulk is metallic as the Fermi energy always crosses some Landau bands. Right: the charge density wave may gap the Landau band, so that the bulk is insulating and the quantum Hall effect can be observed.

electron gas into decoupled 2D quantum Hall layers to realize a 3D quantum Hall effect (Fig. 1, right) [7]. Quite different from the known cases [29–31], the CDW of Landau bands depends on the magnetic field strongly [32–40]. Recently, the CDW mechanism of the 3D quantum Hall effect has been observed in 3D crystals of $ZrTe_5$ [41], providing a platform to study this rare phase of matter where both order parameter and topological number coexist.

In this Letter, we develop a theory for the CDW mechanism of 3D quantum Hall effect. The theory captures the main features in the experiment of $ZrTe_5$ at the quantitative level. We find that electron-phonon interactions dominate the formation of the CDW, instead of electron-electron interactions. We extract electron-phonon coupling constant from the non-Ohmic $I - V$ relation. We point out a crossover between commensurate and incommensurate CDWs, tunable by the magnetic field. More importantly, the theory addresses a rare but experiment-accessible scenario, described by an order parameter along one direction but a topological Chern number in other two directions, both tunable by one magnetic field.

1D Landau band in the quantum limit.—We start with a generic Dirac model [42]

$$
\hat{\mathcal{H}}(\mathbf{k}) = \hbar(v_x k_x \tau_x \otimes \sigma_z + v_y k_y \tau_y \otimes \sigma_0 + v_z k_z \tau_x \otimes \sigma_x)
$$
$$
+ [M_0 + M_1(v_x^2 k_x^2 + v_y^2 k_y^2) + M_z k_z^2]\tau_z \otimes \sigma_0, \quad (1)
$$

where $k_{x/y} = -i\partial_{x/y}$, $\tau_{x,y,z,0}$, and $\sigma_{x,y,z,0}$ are Pauli matrices and unit matrix for orbital and spin degrees of freedom, and $M_{0,1,z}$, $v_{x,y,z}$ are the model parameters. This model can describe various semimetals and insulators [18,43–53]. A uniform z-direction (crystal b direction) magnetic field $\mathbf{B} = (0, 0, B)$ is considered by the Landau gauge vector potential $\mathbf{A} = (-By, 0, 0)$, which shifts k_x to $k_x - eBy/\hbar$, where $-e$ is the electron charge and $\hbar$ is the reduced Planck's constant. The magnetic field splits the energy spectrum into a series of 1D bands of Landau levels, dispersing with k_z [Fig. 2(a)].

We will focus on the quantum limit, in which the Fermi energy E_F crosses only the $n = 0+$ Landau band [56]. At the critical magnetic field B_Q when entering the quantum limit, $E_F = E_{k_z=k_F}^{(0+)} = E_{k_z=0}^{(1)}$, where the Fermi wave vector [57]

$$
k_F = 2\pi^2 \hbar n_0 / eB, \quad (2)
$$

n_0 is carrier density, the energy dispersion of the $n = 0+$ Landau band $E_{k_z}^{(0+)} = \sqrt{(\hbar v_z k_z)^2 + (M_0 + M_\perp/\ell_B^2 + M_z k_z^2)^2}$, $M_\perp = M_1 v_x v_y$, the magnetic length is $\ell_B = \sqrt{\hbar/eB}$, the bottom of the $n = 1$ Landau band $E_{k_z=0}^{(1)} = \sqrt{(M_0 + 3M_\perp/\ell_B^2)^2 + 2v_x v_y \hbar^2/\ell_B^2}$. Using $B_Q = 1.3$ T in the above equations, n_0 is found as

8.87×10^{16} cm^{-3}, comparable with the experiment [41], showing that our model and parameters can capture the noninteracting energy spectrum. At this low carrier density, the pocket at the M point does not contribute [41,58].

Theory of CDW for the Landau band.—We study the CDW of the $0+$ Landau band by using a mean-field approach, which can capture the physics of 1D CDWs [29,30]. Different from previous theories (e.g., [31]), the 1D Landau band here strongly depends on the magnetic field, e.g., the changing k_F in Eq. (2), the nesting momentum k_{cdw}, and CDW wavelength λ_{cdw}.

As shown by the g-ology diagram in Fig. 2(b), the CDW gap (described by the order parameter Δ) can be opened by the coupling between the electrons near k_F and $-k_F$, through either electron-electron or electron-phonon interactions along the z direction. The electron-electron interaction reads [37,40,54,59,60]

$$
\hat{H}_{ee} = -\sum_{\mathbf{k}} |\Delta|(e^{i\phi}\hat{d}_{\mathbf{k}+}^\dagger \hat{d}_{\mathbf{k}-} + \text{H.c.}) + \frac{2|\Delta|^2 V}{U(2k_F)}, \quad (3)
$$

where the order parameter is defined as $\Delta = \Delta_{ee} = [U(2k_F)/2V]\sum_{\mathbf{k}}\langle\hat{d}_{\mathbf{k}-2k_F\mathbf{e}_z}^\dagger \hat{d}_{\mathbf{k}}\rangle$ and V is the volume. $\Delta = |\Delta|e^{i\phi}$, where ϕ is the phase. $\hat{d}_{\mathbf{k}\pm}^\dagger$ and $\hat{d}_{\mathbf{k}\pm}$ are the creation and annihilation operators in the vicinity of $\mp k_F$, respectively, where $\mathbf{k}\pm \equiv k_z \pm k_F$. As shown in Fig. 2(b), the electron-electron potential takes the Yukawa form [61] $U(2k_F) = e^2/\{\epsilon_r\epsilon_0[(2k_F)^2 + \kappa^2]\}$, where ϵ_r (ϵ_0) is the relative (vacuum) dielectric constant and $1/\kappa$ is the screening length. Under the random phase approximation [Fig. 2(b)], we have $\kappa = \sqrt{e^3 B/(4\pi^2\epsilon\hbar^2 v_F)}$ (Eq. (S18) in [59]) with $\epsilon = \epsilon_0\epsilon_r$. The Hamiltonians for electron-phonon interaction and phonons can be, respectively, written as [29,54,62,63]

$$
\hat{H}_{e-ph} = \sum_{\mathbf{k}} |\Delta|(e^{i\phi}\hat{d}_{\mathbf{k}+}^\dagger \hat{d}_{\mathbf{k}-} + \text{H.c.}),
$$
$$
\hat{H}_{ph} = \sum_{\mathbf{q}} \hbar\omega_{\mathbf{q}}\hat{b}_{\mathbf{q}}^\dagger \hat{b}_{\mathbf{q}}, \quad (4)
$$

where $\Delta = \Delta_{e-ph} = (\alpha_{\mathbf{q}}/V)(\langle\hat{b}_{\mathbf{q}}\rangle + \langle\hat{b}_{-\mathbf{q}}^\dagger\rangle)$, $\hat{b}_{\mathbf{q}}^\dagger$ and $\hat{b}_{\mathbf{q}}$ are the creation and annihilation operators for the phonons with momentum $\mathbf{q} = \pm 2k_F\mathbf{e}_z$, the electron-phonon coupling [54] $\alpha_{\mathbf{q}}$ also takes the Yukawa form (Sec. SIV(B) of [59]). Near $\pm k_F$, the mean-field Hamiltonian of the $0+$ Landau band can be written as (Sec. SIV of [59])

$$
\mathcal{H}_{k_z}^{0+} = \begin{pmatrix} \hbar v_F(k_z \pm k_F) & \Delta \\ \Delta^* & -\hbar v_F(k_z \pm k_F) \end{pmatrix}, \quad (5)
$$

where $\hbar v_F \equiv |\partial E_{k_z}^{(0+)}/\partial k_z|_{k_z=k_F}$ (Sec. SIII of [59]). The eigen energies of $\mathcal{H}_{k_z}^{0+}$ can be found as $E_{k_z} = E_F \pm$
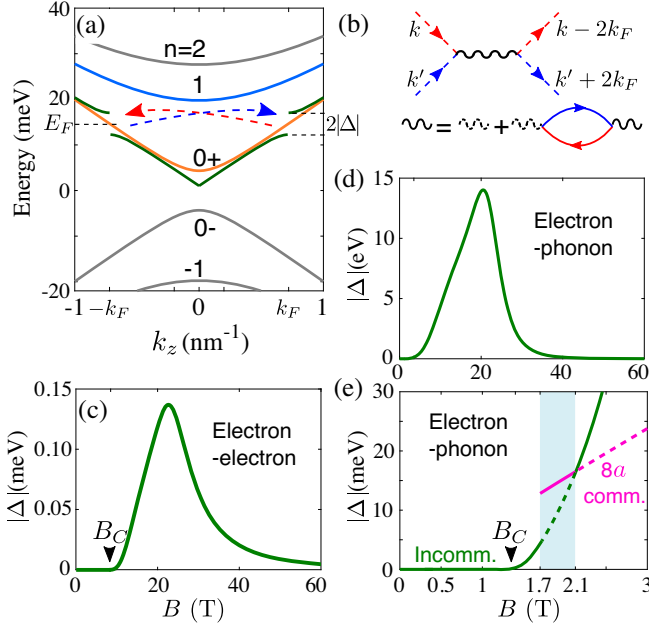
FIG. 2. (a) The 1D energy bands of Landau levels dispersing with the z-direction wave vector k_z in a z-direction magnetic field $B = 1.6$ T. The CDW opens the gap $(2|\Delta|)$ at the Fermi energy E_F. n marks the indices of the Landau bands. $n = 0\pm$ are the lowest Landau bands. (b) Up: the g-ology, which is a diagrammatic representation of the interaction and scattering processes (arrowed $\pm k_F$) involved in the charge density wave and competing phases [30]. Down: the diagrams for the Yukawa potential. The solid wavy line stands for interactions under the random phase approximation [54], the dashed wavy line represents the bare Coulomb interaction, and the solid line represents the bare electronic propagator. (c)–(e) The calculated CDW order parameters for electron-electron (c) and electron-phonon (d),(e) interactions, respectively. B_C indicates a threshold magnetic field at which there is a second-order phase transition as Δ overcomes temperature. "Incomm." and "$8a$ comm." indicate that incommensurate and commensurate (CDW wavelength/lattice constant $= 8$) CDWs are assumed, respectively. The parameters are $v_x = 9 \times 10^5$ m/s, $v_y = 1.9 \times 10^5$ m/s, $v_z = 0.3 \times 10^5$ m/s, $M_0 = -4.7$ meV, $M_\perp = 150$ meV $\cdot$ nm^2, $M_z = 0.01 M_\perp$, $a = 7.25$ Å [41,51], $n_0 = 8.87 \times 10^{16}$ cm^{-3}, $\epsilon_r = 25.3$ [55], and the electron-phonon coupling constant $g_0 = 537.3$ eV $\cdot$ nm^{-1} (determined by comparing with the nonlinear $I - V$ data [41] in Fig. 4(h)), and $T = 0$ K.

$\text{sgn}(k_z \mp k_F) \sqrt{[v_F \hbar (k_z \mp k_F)]^2 + |\Delta|^2}$ near $\pm k_F$ [green curves in Fig. 2(a)], respectively, where $\text{sgn}(x)$ is the sign function.

The CDW order parameter is calculated self-consistently from the gap equation defined by $\partial E_g / \partial |\Delta| = 0$, where the ground-state energy $E_g \equiv \langle \hat{H}_m \rangle$ is found as (Sec. SV of [59])

$$E_g = \sum_{\mathbf{k}} (E_{k_z} - E_F) \Theta(E_F - E_{k_z}) + \frac{|\Delta|^2 V}{g_{2k_F}}, \quad (6)$$

where E_g includes the phonon part, $\Theta(x)$ is the step function, $\hat{H}_m = \sum_{\mathbf{k}} \hat{\Psi}_{\mathbf{k}}^\dagger \mathcal{H}_{k_z}^{0+} \hat{\Psi}_{\mathbf{k}} + |\Delta|^2 V / g_{2k_F}$, $\hat{\Psi}_{\mathbf{k}} \equiv (\hat{d}_{\mathbf{k}+}, \hat{d}_{\mathbf{k}-})^T$, and $\mathcal{H}_{k_z}^{0+}$ has been given in Eq. (5). The coupling $g_{2k_F} = e^2 / \{2\epsilon[(2k_F)^2 + \kappa^2]\}$ for electron-electron interactions and $g_{2k_F} = g_0 / [(2k_F)^2 + \kappa^2]^2$ for electron-phonon interactions with the coupling constant g_0 (Sec. SIV(B) of [59]). The second positive term is from the mean-field phonon Hamiltonian (Eq. (S28) in [59]). As a function of the order parameter, Eq. (6) reduces to a minimum value (GS energy) at a finite gap as shown in Fig. S3 of the Supplemental Material [59]. Different from no-magnetic-field theories, here the summation $\sum_{k_x, k_y} = S_{xy} / (2\pi \ell_B^2)$ gives the Landau degeneracy, with the area S_{xy} in the x–y plane, $V = S_{xy} L_z$, and the length L_z along the z direction.

At extremely low temperatures, i.e., $T \to 0$, the finite-temperature gap equation can be expressed as (Sec. SVI(C) of [59])

$$\int_0^{v_F \hbar k_F} \frac{1}{1 + e^{-E_T(t,\Delta)/k_B T}} \frac{dt}{E_T(t, \Delta)} = \frac{4\pi^2 \hbar^2 v_F}{g_{2k_F} eB}, \quad (7)$$

where $E_T(t, \Delta) = \sqrt{t^2 + |\Delta|^2}$, k_B is the Boltzmann constant, and T is the temperature. We use the Ginzburg criterion [29,64–67] to justify the mean-field approximation at the experimental finite temperatures (Sec. SIV of [59]). Also, we find that the commensurability energy from the ionic potential of the crystal [29,68,69] can be ignored (Sec. SVII of [59]).

Electron-electron or electron-phonon interactions?—As shown in Fig. 2(c), the order parameter calculated using electron-electron interactions is sizable only beyond a threshold magnetic B_C about 10 T, an order larger than those in the experiments [Fig. 3(a)]. On the other hand, for electron-phonon interactions with a proper coupling constant ($g_0 = 537.3$ eV $\cdot$ nm^{-1}, determined by the non-Ohmic $I - V$ relation [Fig. 4(h)]), the threshold B_C could be less than 1.5 T and Δ could be of several to tens of meV [Fig. 2(e)], both consistent with the experiment. Therefore, electron-phonon interactions may be the mechanism in the ZrTe$_5$ experiment.

Commensurate-incommensurate crossover.—In the experiment, the plateau of the Hall resistivity covers a wide range from 1.7 to 2.1 T, which is surprising for the following reason. According to Fig. 1, the Hall conductivity in units of e^2/h is given by the number of the CDW layers $\sigma_{xy} = (e^2/h)/\lambda_{cdw}$ per unit length, where λ_{cdw} is the CDW wavelength, so the height of plateau should be $\rho_{xy} = 1/\sigma_{xy} = (h/e^2)\lambda_{cdw}$ when $\sigma_{xx} = 0$. It is known that the CDW wavelength λ_{cdw} is related to the Fermi wavelength as [29] (Sec. SV of [59])
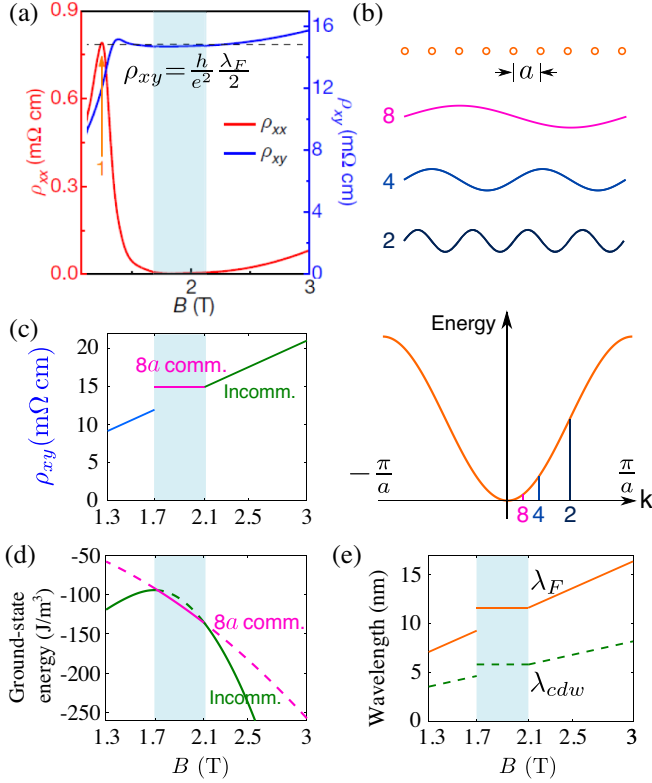
$$\lambda_{cdw} = \lambda_F / 2 = \pi / k_F. \quad (8)$$

FIG. 3. (a) The Hall (ρ_{xy}) and longitudinal (ρ_{xx}) resistivities adapted from the experiment [41]. (b) Schematic of the commensurate CDWs, whose wavelengths are integer times of the lattice constant a. (c) Our understanding to ρ_{xy}. $B \in [1.3, 1.7]$ T, ρ_{xy} is not quantized due to the broadening of the $n = 1$ Landau band bottom [see also Fig. 4(e)]; $B \in [1.7, 2.1]$ T, a commensurate CDW pins λ_{cdw} and λ_F, leading to the plateau of ρ_{xy}; $B \in [2.1, 3]$ T, the incommensurate CDW takes over, so $\rho_{xy} \propto B$. (d) Ground-state energies E_g (per unit volume) of incommensurate and commensurate ($\lambda_{cdw}/a = 8$) CDWs, which shows that the commensurate (incommensurate) CDW has lower energy when $B \in [1.7, 2.1]$([2.1, 3] T). (e) The Fermi (λ_F) and CDW (λ_{cdw}) wavelengthes.

According to Eq. (2), k_F decreases with the magnetic field, leading to a λ_{cdw} linearly increasing with the magnetic field [e.g., $B > 2.1$ T in Fig. 3(e)], so ρ_{xy} should increase linearly with B. That is why the plateau in Fig. 3(a) is surprising.

The observed ρ_{xy} plateau between 1.7 and 2.1 T implies that there is a commensurate CDW, i.e., the CDW wavelength is pinned at integer times of the lattice constant a [Fig. 3(b)]. According to the experiment, $\lambda_{cdw}/a = 8.1 \pm 0.8$ [41]. We compare the ground-state energies of commensurate ($\lambda_{cdw}/a = 8$) and incommensurate CDWs near 2.1 T, which can be obtained by minimizing the ground-state energy E_g in Eq. (6). As shown in Fig. 3(d), the commensurate (incommensurate) CDW has lower energy for $B \in [1.7, 2.1]$([2.1, 3]) T, so there is a crossover between the commensurate and incommensurate CDWs [$B = 2.1$ T in Fig. 3(c)]. In the range $B \in [1.7, 2.1]$ T, the fixed λ_{cdw} means a fixed Fermi energy, i.e., the system is

a grand canonical ensemble and the number of carriers can change. By contrast, the number of carriers in the incommensurate CDW phase cannot change. Therefore, the change of electrons leads to lower ground-state energy of the commensurate CDW phase in the range $B \in [1.7, 2.1]$ T. Further increasing the magnetic field above 2.1 T, the magnetic field will push the Fermi energy lower (eventually to the band bottom), so there is a crossover from commensurate to incommensurate CDW phase as a function of the magnetic field. These are unique properties of this magnetic field–induced CDW.

Non-Ohmic $I - V$ relation.—An evidence of CDW is the non-Ohmic $I - V$ relation [70,71], because a bias voltage has to overcome the barriers of CDW [Fig. 4(a)], which can be used to determine Δ and more importantly the electron-phonon interaction coupling constant g_0 by comparing with our theory. The tunneling current I_{cdw} is found as [29,72]

$$I_{cdw} = \frac{e}{h}|\mathcal{T}|^2 \int_{-\infty}^{\infty} d\epsilon D_{cdw}(\epsilon) D_N(\epsilon + eV_z)$$
$$\times [f(\epsilon) - f(\epsilon + eV_z)], \tag{9}$$

with the density of states [Fig. 4(b)] $D_{cdw}(E_{k_z})/D_N(0) = |E_{k_z} - E_F|\Theta(|E_{k_z} - E_F| - |\Delta|)/\sqrt{(E_{k_z} - E_F)^2 - |\Delta|^2}$ (Sec. SVIII(A) of [59]), where the normal (N) density of states $D_N(0)$ and tunneling matrix element $\mathcal{T}$ are assumed energy independent, and $f(x) = 1/[1 + e^{x/(k_B T)}]$ is the Fermi function [73]. Figure 4(c) shows the non-Ohmic $I_{cdw} - V_z$ relation at different temperatures. At zero temperature, there is no tunneling current below the threshold voltage $V_{th} \equiv |\Delta|/e$. Finite temperatures can lead to a small tunneling current for $|V_z| < V_{th}$. Figure 4(d) shows the differential conductance dI_{cdw}/dV_z as a function of V_z at different temperatures, where the peak near the threshold V_{th} at $T = 2.5$ K is due to the abrupt increase of I_{cdw} across the threshold and is smeared at higher temperatures.

Figure 4(h) shows the differential resistance dV_z/dI_z in the experiment [41]. There is a plateau below the threshold current $I_{th} \approx 450 \mu A$, besides the non-Ohmic behavior above I_{th}. This implies that besides the $0+$ Landau band, there is another Ohmic channel, likely the broadened $+1$ band bottom which lasts till $B = 1.7$ T [Fig. 4(e)]. Therefore, we model the current as $I_z = I_{cdw} + I_N$ [63,74], where I_{cdw} is the CDW current from the $0+$ band and the normal band is assumed to satisfy the Ohmic law $I_N = G_N V_z$. We reproduce the Ohmic plateau and non-Ohmic $I_z - V_z$ relation at different temperatures [Fig. 4(g)]. Using I_{th} in the experiment, we find that $g_0 = 537.3$ eV · nm^{-1}. For $T = 1.5$ K, we assume that $I_z = I_{cdw}^{(1)}(T) + I_N^{(1)}$ for $I_z < I_{th}$ and $I_z = I_{cdw}^{(2)}(\alpha_1 T) + I_N^{(2)}$ for $I_z > I_{th}$; for $T = 2.5$ K, $I_z = I_{cdw}^{(3)}(\alpha_2 T) + I_N^{(3)}$, where $\alpha_{1,2}$ describe the Joule heat from the abrupt current
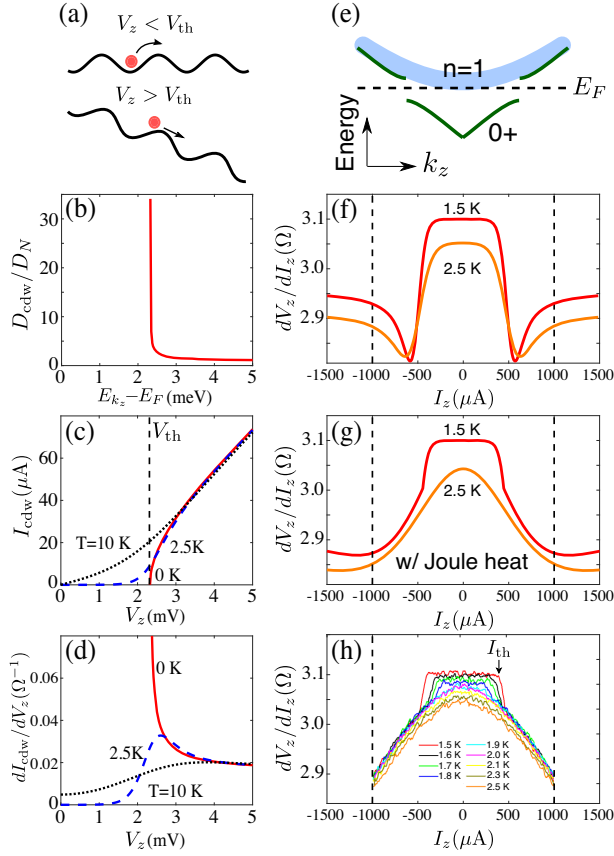
FIG. 4. (a) A bias voltage V_z has to overcome the threshold voltage V_{th} of CDW to yield a current, leading to the non-Ohmic $I - V$ relation. (b)–(d) At $B = 1.6$ T, CDW density of states (b), non-Ohmic relation between the tunneling current I_{cdw} and V_z (c), and differential conductance dI_{cdw}/dV_z (d). (e) At $B = 1.55$ T, the Fermi energy E_F is assumed to cross both the CDW-gapped $n = 0+$ and broadened $n = 1$ Landau bands. (f), (g) Differential resistance dV_z/dI_z as a function of the z-direction current at $B = 1.55$ T and different temperatures, without (f) and assuming the Joule heat (g). The parameters $\alpha_1 = 7$, $G_{cdw}^{(1)} = 322.58$ mΩ^{-1}, $G_N^{(1)} = 16.64$ mΩ^{-1}, $G_{cdw}^{(2)} = 293.25$ mΩ^{-1}, and $G_N^{(2)} = 49.75$ mΩ^{-1} at $T = 1.5$ K; $\alpha_2 = 5$, $G_{cdw}^{(3)} = 294.12$ mΩ^{-1}, and $G_N^{(3)} = 53.76$ mΩ^{-1} at $T = 2.5$ K. (h) Experimental data of dV_z/dI_z [41].

increase. Without the Joule heat, dV_z/dI_z shows a dip near I_{th} [Fig. 4(f)], due to the dI_{cdw}/dV_z peak in Fig. 4(d).

Discussions and perspectives.—At higher magnetic fields, signatures of fractional quantum Hall effect have been reported [41,75], which is a promising topic. At lower magnetic fields ($B \in [0.6, 1]$ T), the experiment also shows some plateaulike behaviors in the Hall resistivity [41], implying a simultaneous CDW phase of multiple bands. The CDW mechanism of 3D quantum Hall effect could be realized also in layered structures HfTe$_5$, TaS$_2$, NbSe$_3$, etc. In Type-II Weyl semimetals [38], the overtilted pockets may lead to a cascade of CDW and even multiple 3D Hall plateaus for weak interactions.

---

*Corresponding author.
luhz@sustech.edu.cn

[1] K. v. Klitzing, G. Dorda, and M. Pepper, New Method for High-Accuracy Determination of the Fine-Structure Constant Based on Quantized Hall Resistance, Phys. Rev. Lett. **45**, 494 (1980).

[2] D. C. Tsui, H. L. Stormer, and A. C. Gossard, Two-Dimensional Magnetotransport in the Extreme Quantum Limit, Phys. Rev. Lett. **48**, 1559 (1982).

[3] R. B. Laughlin, Anomalous Quantum Hall Effect: An Incompressible Quantum Fluid with Fractionally Charged Excitations, Phys. Rev. Lett. **50**, 1395 (1983).

[4] D. J. Thouless, M. Kohmoto, M. P. Nightingale, and M. den Nijs, Quantized Hall Conductance in a Two-Dimensional Periodic Potential, Phys. Rev. Lett. **49**, 405 (1982).

[5] Y. Zhang, Y.-W. Tan, H. L. Stormer, and P. Kim, Experimental observation of the quantum Hall effect and Berry's phase in graphene, Nature (London) **438**, 201 (2005).

[6] H.-Z. Lu, Perspective: 3D quantum Hall effect, Natl. Sci. Rev. **6**, 208 (2019).

[7] B. I. Halperin, Possible states for a three-dimensional electron gas in a strong magnetic field, Jpn. J. Appl. Phys. **26**, 1913 (1987).

[8] G. Montambaux and M. Kohmoto, Quantized Hall effect in three dimensions, Phys. Rev. B **41**, 11417 (1990).

[9] M. Kohmoto, B. I. Halperin, and Y.-S. Wu, Diophantine equation for the three-dimensional quantum Hall effect, Phys. Rev. B **45**, 13488 (1992).

[10] M. Koshino, H. Aoki, K. Kuroki, S. Kagoshima, and T. Osada, Hofstadter Butterfly and Integer Quantum Hall Effect in Three Dimensions, Phys. Rev. Lett. **86,** 1062 (2001).

[11] B. A. Bernevig, T. L. Hughes, S. Raghu, and D. P. Arovas, Theory of the Three-Dimensional Quantum Hall Effect in Graphite, Phys. Rev. Lett. **99,** 146804 (2007).

[12] H. L. Störmer, J. P. Eisenstein, A. C. Gossard, W. Wiegmann, and K. Baldwin, Quantization of the Hall Effect in an Anisotropic Three-Dimensional Electronic System, Phys. Rev. Lett. **56,** 85 (1986).

[13] J. R. Cooper, W. Kang, P. Auban, G. Montambaux, D. Jérome, and K. Bechgaard, Quantized Hall Effect and a New Field-Induced Phase Transition in the Organic Superconductor $(TMTSF)_2PF_6$, Phys. Rev. Lett. **63,** 1984 (1989).

[14] S. T. Hannahs, J. S. Brooks, W. Kang, L. Y. Chiang, and P. M. Chaikin, Quantum Hall Effect in a Bulk Crystal, Phys. Rev. Lett. **63,** 1988 (1989).

[15] S. Hill, S. Uji, M. Takashita, C. Terakura, T. Terashima, H. Aoki, J. S. Brooks, Z. Fisk, and J. Sarrao, Bulk quantum Hall effect in η-Mo_4O_{11}, Phys. Rev. B **58,** 10778 (1998).

[16] H. Cao, J. Tian, I. Miotkowski, T. Shen, J. Hu, S. Qiao, and Y. P. Chen, Quantized Hall effect and Shubnikov–de Haas Oscillations in Highly Doped Bi_2Se_3: Evidence for Layered Transport of Bulk Carriers, Phys. Rev. Lett. **108,** 216803 (2012).

[17] H. Masuda, H. Sakai, M. Tokunaga, Y. Yamasaki, A. Miyake, J. Shiogai, S. Nakamura, S. Awaji, A. Tsukazaki, H. Nakao, Y. Murakami, T.-h. Arima, Y. Tokura, and S. Ishiwata, Quantum Hall effect in a bulk antiferromagnet $EuMnBi_2$ with magnetically confined two-dimensional Dirac fermions, Sci. Adv. **2,** e1501117 (2016).

[18] Y. Liu, X. Yuan, C. Zhang, Z. Jin, A. Narayan, C. Luo, Z. Chen, L. Yang, J. Zou, X. Wu, S. Sanvito, Z. Xia, L. Li, Z. Wang, and F. Xiu, Zeeman splitting and dynamical mass generation in Dirac semimetal $ZrTe_5$, Nat. Commun. **7,** 12516 (2016).

[19] C. M. Wang, H.-P. Sun, H.-Z. Lu, and X. C. Xie, 3D Quantum Hall Effect of Fermi Arcs in Topological Semimetals, Phys. Rev. Lett. **119,** 136806 (2017).

[20] C. Zhang, E. Zhang, W. Wang, Y. Liu, Z.-G. Chen, S. Lu, S. Liang, J. Cao, X. Yuan, L. Tang, Q. Li, C. Zhou, T. Gu, Y. Wu, J. Zou, and F. Xiu, Room-temperature chiral charge pumping in Dirac semimetals, Nat. Commun. **8,** 13741 (2017).

[21] M. Uchida, Y. Nakazawa, S. Nishihaya, K. Akiba, M. Kriener, Y. Kozuka, A. Miyake, Y. Taguchi, M. Tokunaga, N. Nagaosa et al., Quantum Hall states observed in thin films of Dirac semimetal Cd_3As_2, Nat. Commun. **8,** 2274 (2017).

[22] T. Schumann, L. Galletti, D. A. Kealhofer, H. Kim, M. Goyal, and S. Stemmer, Observation of the Quantum Hall Effect in Confined Films of the Three-Dimensional Dirac Semimetal Cd_3As_2, Phys. Rev. Lett. **120,** 016801 (2018).

[23] C. Zhang, Y. Zhang, X. Yuan, S. Lu, J. Zhang, A. Narayan, Y. Liu, H. Zhang, Z. Ni, R. Liu, E. S. Choi, A. Suslov, S. Sanvito, L. Pi, H.-Z. Lu, A. C. Potter, and F. Xiu, Quantum Hall effect based on Weyl orbit in Cd_3As_2, Nature (London) **565,** 331 (2019).

[24] J. Y. Liu et al., Spin-valley locking, bulk quantum Hall effect and chiral surface state in a noncentrosymmetric Dirac semimetal $BaMnSb_2$, arXiv:1907.06318.

[25] H. Li, H. Liu, H. Jiang, and X. C. Xie, 3d Quantum Hall Effect and a Global Picture of Edge States in Weyl Semimetals, Phys. Rev. Lett. **125,** 036602 (2020).

[26] S.-g. Cheng, H. Jiang, Q.-F. Sun, and X. C. Xie, Quantum Hall effect in wedge-shaped samples, Phys. Rev. B **102,** 075304 (2020).

[27] P. Wang, Y. Ren, F. Tang, P. Wang, T. Hou, H. Zeng, L. Zhang, and Z. Qiao, Approaching three-dimensional quantum hall effect in bulk $HfTe_5$, Phys. Rev. B **101,** 161201(R) (2020).

[28] R. Ma, D. N. Sheng, and L. Sheng, Three-dimensional quantum hall effect and magnetothermoelectric properties in weyl semimetals, arXiv:2008.13431.

[29] G. Grüner, Density Waves in Solids (Perseus, Cambridge, 2000).

[30] T. Giamarch, Quantum Physics in One Dimension (Oxford University Press, Oxford, 2004).

[31] P. A. Lee and T. M. Rice, Electric field depinning of charge density waves, Phys. Rev. B **19,** 3970 (1979).

[32] V. Celli and N. D. Mermin, Ground state of an electron gas in a magnetic field, Phys. Rev. **140,** A839 (1965).

[33] V. M. Yakovenko, Metals in a high magnetic field: A universality class of marginal Fermi liquids, Phys. Rev. B **47,** 8851 (1993).

[34] G. Möller and N. R. Cooper, Density Waves and Super-solidity in Rapidly Rotating Atomic Fermi Gases, Phys. Rev. Lett. **99,** 190409 (2007).

[35] X.-T. Zhang and R. Shindou, Transport properties of density wave phases in three-dimensional metals and semimetals under high magnetic field, Phys. Rev. B **95,** 205108 (2017).

[36] K. Y. Yang, Y. M. Lu, and Y. Ran, Quantum Hall effects in a Weyl semimetal: Possible application in pyrochlore iridates, Phys. Rev. B **84,** 075129 (2011).

[37] Z. Song, Z. Fang, and X. Dai, Instability of Dirac semimetal phase under a strong magnetic field, Phys. Rev. B **96,** 235104 (2017).

[38] M. Trescher, E. J. Bergholtz, M. Udagawa, and J. Knolle, Charge density wave instabilities of type-II weyl semimetals in a strong magnetic field, Phys. Rev. B **96,** 201101(R) (2017).

[39] M. Trescher, E. J. Bergholtz, and J. Knolle, Quantum oscillations and magnetoresistance in type-II weyl semimetals: Effect of a field-induced charge density wave, Phys. Rev. B **98,** 125304 (2018).

[40] Z. Pan and R. Shindou, Ground-state atlas of a three-dimensional semimetal in the quantum limit, Phys. Rev. B **100,** 165124 (2019).

[41] F. Tang, Y. Ren, P. Wang, R. Zhong, J. Schneeloch, S. A. Yang, K. Yang, P. A. Lee, G. Gu, Z. Qiao, and L. Zhang, Three-dimensional quantum Hall effect and metal-insulator transition in $ZrTe_5$, Nature (London) **569,** 537 (2019).

[42] R. Y. Chen, Z. G. Chen, X.-Y. Song, J. A. Schneeloch, G. D. Gu, F. Wang, and N. L. Wang, Magnetoinfrared Spectroscopy of Landau Levels and Zeeman Splitting of Three-Dimensional Massless Dirac Fermions in $ZrTe_5$, Phys. Rev. Lett. **115,** 176404 (2015).

[43] H. Weng, X. Dai, and Z. Fang, Transition-Metal Pentatelluride ZrTe$_5$ and HfTe$_5$: A Paradigm for Large-Gap Quantum Spin Hall Insulators, Phys. Rev. X **4**, 011002 (2014).

[44] Z. Fan, Q.-F. Liang, Y. B. Chen, S.-H. Yao, and J. Zhou, Transition between strong and weak topological insulator in ZrTe$_5$ and HfTe$_5$, Sci. Rep. **7**, 45667 (2017).

[45] G. Manzoni, L. Gragnaniello, G. Autès, T. Kuhn, A. Sterzi, F. Cilento, M. Zacchigna, V. Enenkel, I. Vobornik, L. Barba, F. Bisti, P. Bugnon, A. Magrez, V. N. Strocov, H. Berger, O. V. Yazyev, M. Fonin, F. Parmigiani, and A. Crepaldi, Evidence for a Strong Topological Insulator Phase in ZrTe$_5$, Phys. Rev. Lett. **117**, 237601 (2016).

[46] R. Y. Chen, S. J. Zhang, J. A. Schneeloch, C. Zhang, Q. Li, G. D. Gu, and N. L. Wang, Optical spectroscopy study of the three-dimensional Dirac semimetal ZrTe$_5$, Phys. Rev. B **92**, 075107 (2015).

[47] N. L. Nair, P. T. Dumitrescu, S. Channa, S. M. Griffin, J. B. Neaton, A. C. Potter, and J. G. Analytis, Thermodynamic signature of Dirac electrons across a possible topological transition in ZrTe$_5$, Phys. Rev. B **97**, 041111(R) (2018).

[48] Q. Li, D. E. Kharzeev, C. Zhang, Y. Huang, I. Pletikosic, A. V. Fedorov, R. D. Zhong, J. A. Schneeloch, G. D. Gu, and T. Valla, Chiral magnetic effect in ZrTe$_5$, Nat. Phys. **12**, 550 (2016).

[49] X.-B. Li, W.-K. Huang, Y.-Y. Lv, K.-W. Zhang, C.-L. Yang, B.-B. Zhang, Y. B. Chen, S.-H. Yao, J. Zhou, M.-H. Lu, L. Sheng, S.-C. Li, J.-F. Jia, Q.-K. Xue, Y.-F. Chen, and D.-Y. Xing, Experimental Observation of Topological Edge States at the Surface Step Edge of the Topological Insulator ZrTe$_5$, Phys. Rev. Lett. **116**, 176803 (2016).

[50] Z.-G. Chen, R. Y. Chen, R. D. Zhong, J. Schneeloch, C. Zhang, Y. Huang, F. Qu, R. Yu, Q. Li, G. D. Gu, and N. L. Wang, Spectroscopic evidence for bulk-band inversion and three-dimensional massive Dirac fermions in ZrTe$_5$, Proc. Natl. Acad. Sci. U.S.A. **114**, 816 (2017).

[51] Y. Jiang, Z. L. Dun, H. D. Zhou, Z. Lu, K.-W. Chen, S. Moon, T. Besara, T. M. Siegrist, R. E. Baumbach, D. Smirnov, and Z. Jiang, Landau-level spectroscopy of massive Dirac fermions in single-crystalline ZrTe$_5$ thin flakes, Phys. Rev. B **96**, 041101(R) (2017).

[52] H. Xiong, J. A. Sobota, S.-L. Yang, H. Soifer, A. Gauthier, M.-H. Lu, Y.-Y. Lv, S.-H. Yao, D. Lu, M. Hashimoto, P. S. Kirchmann, Y.-F. Chen, and Z.-X. Shen, Three-dimensional nature of the band structure of ZrTe$_5$ measured by high-momentum-resolution photoemission spectroscopy, Phys. Rev. B **95**, 195119 (2017).

[53] B. Xu, L. X. Zhao, P. Marsik, E. Sheveleva, F. Lyzwa, Y. M. Dai, G. F. Chen, X. G. Qiu, and C. Bernhard, Temperature-Driven Topological Phase Transition and Intermediate Dirac Semimetal Phase in ZrTe$_5$, Phys. Rev. Lett. **121**, 187401 (2018).

[54] H. Bruus and K. Flensberg, *Many-Body Quantum Theory in Condensed Matter Physics: An Introduction* (Oxford University Press, Oxford, 2004).

[55] Y. Hochberg, Y. Kahn, M. Lisanti, K. M. Zurek, A. G. Grushin, R. Ilan, S. M. Griffin, Z.-F. Liu, S. F. Weber, and J. B. Neaton, Detection of sub-MeV dark matter with three-dimensional Dirac materials, Phys. Rev. D **97**, 015004 (2018).

[56] G. Zheng, J. Lu, X. Zhu, W. Ning, Y. Han, H. Zhang, J. Zhang, C. Xi, J. Yang, H. Du, K. Yang, Y. Zhang, and M. Tian, Transport evidence for the three-dimensional Dirac semimetal phase in ZrTe$_5$, Phys. Rev. B **93**, 115414 (2016).

[57] H. Z. Lu, S. B. Zhang, and S. Q. Shen, High-field magneto-conductivity of topological semimetals with short-range potential, Phys. Rev. B **92**, 045203 (2015).

[58] J. L. Zhang, C. M. Wang, C. Y. Guo, X. D. Zhu, Y. Zhang, J. Y. Yang, Y. Q. Wang, Z. Qu, L. Pi, H.-Z. Lu, and M. L. Tian, Anomalous Thermoelectric Effects of ZrTe$_5$ in and Beyond the Quantum Limit, Phys. Rev. Lett. **123**, 196602 (2019).

[59] See Supplemetal Material at http://link.aps.org/supplemental/10.1103/PhysRevLett.125.206601 for detailed calculations, which includes Refs. [29,30,37, 40–42,51,54,58,60–74].

[60] R. A. Jishi, *Feynman Diagram Techniques in Condensed Matter Physics* (Cambridge University Press, Cambridge, United Kingdom, 2013).

[61] A. A. Abrikosov, Quantum magnetoresistance, Phys. Rev. B **58**, 2788 (1998).

[62] B. Roy, J. D. Sau, and S. Das Sarma, Migdal's theorem and electron-phonon vertex corrections in Dirac materials, Phys. Rev. B **89**, 165119 (2014).

[63] G. Grüner, The dynamics of charge-density waves, Rev. Mod. Phys. **60**, 1129 (1988).

[64] A. P. Levanyuk, Contribution to the theory of light scattering near the second-order phase transition points, J. Exp. Theor. Phys. **36**, 571 (1959).

[65] V. L. Ginzburg, Some remarks on phase transitions of the second kind and the microscopic theory of ferroelectrics, J. Exp. Theor. Phys. **2**, 1824 (1960).

[66] P. Coleman, *Introduction to Many-Body Physics* (Cambridge University Press, Cambridge, United Kingdom, 2015).

[67] P. A. Lee, T. M. Rice, and P. W. Anderson, Fluctuation Effects at a Peierls Transition, Phys. Rev. Lett. **31**, 462 (1973).

[68] P. A. Lee, T. M. Rice, and P. W. Anderson, Conductivity from charge or spin density waves, Solid State Commun. **14**, 703 (1974).

[69] S. Kagoshima, H. Nagasawa, and T. Sambongi, *One-Dimensional Conductors* (Springer, Berlin, Heidelberg, 1988).

[70] J. Bardeen, Theory of Non-Ohmic Conduction from Charge-Density Waves in NbSe$_3$, Phys. Rev. Lett. **42**, 1498 (1979).

[71] J. Bardeen, Tunneling Theory of Charge-Density-Wave Depinning, Phys. Rev. Lett. **45**, 1978 (1980).

[72] G. D. Mahan, *Many-Particle Physics*, 3rd ed., Physics of Solids and Liquids (Springer Science & Business Media, New York, 2000).

[73] R. K. Pathria, *Statistical Mechanics*, 2nd ed. (Butterworth-Heinemann, Oxford, 1996).

[74] G. Grüner and A. Zettl, Charge density wave conduction: A novel collective transport phenomenon in solids, Phys. Rep. **119**, 117 (1985).

[75] S. Galeski, X. Zhao, R. Wawrzynczak, T. Meng, T. Forster, S. Honnali, N. Lamba, T. Ehmcke, A. Markou, W. Zhu, J. Wosnitza, C. Felser, G. F. Chen, and J. Gooth, Observation of a three-dimensional fractional hall response in HfTe$_5$, arXiv:2003.07213.